Robust numerical schemes for Eulerian spray DNS and LES in two-phase turbulent flows

By M. Boileau†, C. Chalons†, F. Laurent†, S. de Chaisemartin‡ and M. Massot†

Large Eddy Simulation (LES) and Direct numerical Simulation (DNS) of polydisperse evaporating sprays with Eulerian models are very promising tools for high performance computing of combustion applications. However, the spray system of conservation equations has a convective part which is either similar to general gas dynamics (GGD) Euler equations with a real gas type state law or to the pressureless gas dynamics (PGD), depending on the local flow regime and droplet Stokes number; henceforth, it usually features singularities due to model closure assumptions and requires dedicated numerical schemes. Here, we introduce a new generation of numerical methods based on relaxation schemes which are able to treat both PGD and GGD, as well as to cope in a robust manner with droplet vacuum zones and natural singularities of the resulting system of conservation equations. The proposed hybrid relaxation scheme and algorithms are validated through comparisons with analytical solutions and other numerical strategies in 1D and 2D configurations. They exhibit a very robust behavior and are a promising candidate for more complex applications since they provide solutions to key numerical issues of the actual Eulerian spray DNS and LES models.

1. Introduction

Many industrial devices involve turbulent combustion of a liquid fuel. The transportation sector, rocket, aircraft or car engines are almost exclusively based on storage and injection of a liquid phase, which is sprayed into a combustion chamber. To optimize such devices, it is of primary importance to understand and control the physical process as a whole, from the injection into the chamber up to the combustion phenomena. Dealing with the description of the polydisperse spray dynamics, some promising advances have been performed in the field of spray combustion in real devices (Boileau *et al.* (2008); Vié *et al.* (2010)). However, the reliable prediction of such complex two-phase reacting flows requires further work in the modeling of the triple spray/turbulence/combustion interaction, in particular to describe the turbulent spray dispersion. Spray models have a common basis at the mesoscopic level under the form of a number density function (NDF) satisfying a Boltzmann type equation, the so-called Williams equation. Such a transport equation describes the evolution of the NDF of the spray due to convection, heating, evaporation and drag force from the gaseous phase and droplet-droplet interactions. A Lagrangian approach using Direct Simulation Monte-Carlo method is generally considered to be the most accurate for solving Williams equation. However, this method requires a delicate coupling between the disperse and gaseous phase, dedicated algorithms to be efficient in massively parallel calculations as well as high memory and CPU costs

† Laboratoire EM2C-CNRS UPR 288, Ecole Centrale Paris, 92295 Châtenay-Malabry, France
‡ IFP Énergies nouvelles, 1 & 4 avenue de Bois-Prau, 92852 Rueil-Malmaison Cedex - France

to describe the spray polydispersion. An Eulerian formulation for the disperse phase is thus more attractive for massively parallel simulations of industrial configurations.

Kaufmann *et al.* (2008) have proposed a formalism that accounts for the random-uncorrelated motion due to trajectory crossing of inertial particles in the context of DNS and that has been extended to LES by Riber *et al.* (2005). The LES filtering introduces stress, and more specifically a pressure-like term, in the spray conservation equations so that the resulting Eulerian equations for inertial particles dynamics are similar to the GGD equations. In particular, they include a real gas type state law which can eventually degenerate in some parts of the flow to a zero pressure term leading to the peculiar PGD. The main difficulty of the resulting system of conservation equations is related to transport in physical space, that is the convective part of the system, which is either hyperbolic or weakly hyperbolic, and thus leads to singularity formation. In the framework of the PGD system, de Chaisemartin (2009) has solved the problem by using a numerical strategy based on the kinetic scheme of Bouchut which leads to a second order method in space and time with very limited diffusion Freret *et al.* (2011). This numerical scheme captures delta-shocks in density and *vacuum* states which naturally emerge from the weakly hyperbolic system (by *vacuum* states, we denote voids of droplets, that is flow locations where only gas is to be found and the droplet number density is zero). However, this strategy cannot be naturally extended to GGD with arbitrary state laws.

Therefore, the numerical method we are looking for must have the ability 1) to handle an Euler-type system of equations in regions of high Stokes number or in regions where sub-grid scales induce significant pressure effects, 2) to degenerate to the PGD system in regions of Stokes number below the critical value for trajectory crossing and in regions where the subgrid scales do not play any role in particle velocity dispersion, 3) to treat exact vacuum regions for both PGD and GGD systems. Moreover, this method must feature the same properties of robustness with singularities and vacuum treatment as the Bouchut's kinetic scheme for PGD proposed in de Chaisemartin (2009). Finally, since the pressure law can bear some real gas effects, the numerical method has to handle such cases while keeping a high level of accuracy as required by the DNS/LES approach.

In that context, the purpose of the present paper is to introduce a novel numerical method based on relaxation schemes which has the ability to match all the previous requirements. Relaxation methods, introduced in Jin & Xin (1995), and further developed in Suliciu (1998) and Coquel & Perthame (1998), have a common basis: they introduce auxiliary variables in the framework of Godunov schemes in order to treat more easily the strong non-linearity due to the treatment of pressure and state law. They avoid to use complex non-linear Riemann solvers or their approximated versions which can have a very high computational cost with non-standard pressure laws. The non-linearity treatment is replaced by a splitting like strategy in the framework of a linearly degenerate version of the transport step, along with a relaxation step.

In this contribution, we conduct three new steps : 1) extending the work of Berthon *et al.* (2006), we propose a scheme for PGD based on successive energy and pressure relaxation which can deal with vacuum, 2) based on this new scheme, we introduce a hybrid numerical method which can treat both regions with and without pressure and still remain accurate and robust, 3) we finally prove the potential of these schemes by comparing them to standard approaches on 1D and 2D test-cases. Since relaxation methods are able to treat arbitrary state law, we only provide the schemes in the framework of ideal gas law; besides we focus on the purely convective part of the system of conservation laws and do not treat the stress tensors which can be handled by standard schemes.

2. Eulerian modeling of turbulent spray dynamics

At the *mesoscopic* level, spray models have a common basis called the *kinetic model* by analogy with kinetic theory of gases. The spray is described as a statistical cloud of point particles experimenting exchanges of mass, momentum and heat with the carrier phase using a Boltzmann type equation (the Williams equation) for the number density function (NDF) f of the spray, where $f(t,\mathbf{x},\mathbf{u})\mathrm{d}\mathbf{x}\mathrm{d}\mathbf{u}$ denotes the probable number of particles at time t, in a volume of size $\mathrm{d}\mathbf{x}$ around $\mathbf{x}$, with a velocity in a $\mathrm{d}\mathbf{u}$-neighbourhood of $\mathbf{u}$. For sake of simplicity, constant particle size (monodisperse spray) and temperature are considered here so these variables will not appear in the equations. A way to solve the Williams equation is to write conservation equations for the zero and first order moments of the f with respect to the velocity variable at a given time t and position $\mathbf{x}$. These two moments corresponds to the particle density number n and the particle mean velocity $\overline{\mathbf{u}}$ respectively. There are two different ways of deriving the conservation equations for these two moments according to the value of the particle Stokes number St, defined by: $\mathrm{St} = \tau_p/\tau_K$, where τ_K is the Kolmogorov time microscale and τ_p is the particle relaxation time. For low Stokes numbers, particles have a low inertia and do not experience trajectory crossing. Accordingly, the velocity dispersion around the averaged velocity $\overline{\mathbf{u}}(t,\mathbf{x})$ is assumed to be zero in each direction – the spray is called *mono-kinetic* – and the NDF writes $f(t,\mathbf{x},\mathbf{u}) = n(t,\mathbf{x})\delta(\mathbf{u}-\overline{\mathbf{u}}(t,\mathbf{x}))$. Such an assumption leads to the following closed system of conservation equations

$$\left\{\begin{array}{rl} \partial_t n + \partial_{\mathbf{x}}\cdot(n\overline{\mathbf{u}}) & = 0, \\ \partial_t(n\,\overline{\mathbf{u}}) + \partial_{\mathbf{x}}\cdot(n\,\overline{\mathbf{u}}\otimes\overline{\mathbf{u}}) & = n\overline{\mathbf{F}}, \end{array}\right. \tag{2.1}$$

where $\overline{\mathbf{F}}$ is the mean drag force given by the Stokes law $\overline{\mathbf{F}}(t,\mathbf{x},\overline{\mathbf{u}}) = (\mathbf{U}(t,\mathbf{x})-\overline{\mathbf{u}})/\tau_p$, where $\mathbf{U}$ is the gas velocity at the particle location. Equation (2.1) is similar to the PGD system with an additional velocity relaxation source term.

A way to account for the uncorrelated motion of inertial particles is to use the mesoscopic formalism proposed by Fevrier *et al.* (2005), starting from the following decomposition: $\mathbf{u} = \overline{\mathbf{u}}(t,\mathbf{x}) + \delta\mathbf{u}$, where $\delta\mathbf{u}$ is called the random uncorrelated component of the particle velocity. System (2.1), obtained for a mono-kinetic spray, now becomes (see Kaufmann *et al.* (2008)):

$$\left\{\begin{array}{rcl} \partial_t n + \partial_{\mathbf{x}}\cdot(n\overline{\mathbf{u}}) & = & 0 \\ \partial_t(n\overline{\mathbf{u}}) + \partial_{\mathbf{x}}\cdot(n\overline{\mathbf{u}}\otimes\overline{\mathbf{u}}+\mathcal{P}) & = & n\overline{\mathbf{F}} + \partial_{\mathbf{x}}\delta\tau \\ \partial_t(n\mathcal{E}) + \partial_{\mathbf{x}}\cdot(n\mathcal{E}\,\overline{\mathbf{u}}+\mathcal{P}\,\overline{\mathbf{u}}) & = & n\overline{\mathbf{F}}\cdot\overline{\mathbf{u}} - \frac{2n}{\tau}\delta\theta + \mathcal{A} \end{array}\right. \tag{2.2}$$

where the total energy reads $\mathcal{E} = \overline{\mathbf{u}}\cdot\overline{\mathbf{u}}/2 + \delta\theta$, with $\delta\theta$ the random uncorrelated energy (RUE) — defined as half the trace of the random uncorrelated stress tensor — and where $\delta\tau$ is the deviatoric part of the random uncorrelated motion tensor (usually modeled by a viscosity assumption), $\mathcal{P}$ is called the random uncorrelated pressure which is linked to the RUE through the equation of state $\mathcal{P} = 2/3n\,\delta\theta$ and $\mathcal{A}$ contains additional terms described in Kaufmann *et al.* (2008). These equations correspond to the case where the gas flow is entirely resolved and no modeling of the gas turbulence is used (DNS approach). In the context of statistical (RANS) or LES filtering, the pressure law becomes more complicated, involving contributions from turbulent or subgrid motion respectively.

The simplified general form of the system of conservation equation finally considered in the following is then system (2.2) with $\delta\tau = 0$, without the additional terms $\mathcal{A}$ but

with a potential source term, that is $2n/\tau\,\delta\theta$ is replaced by $2n/\tau(\delta\theta - \varepsilon_t)$, where ε_t is the energy source term due to subgrid turbulence agitation. From a numerical point of view, we thus isolate the difficulties of solving system (2.2) which requires numerical method for highly compressible flows. The additional source terms and second order derivatives usually do not lead to numerical difficulties and can be treated through operator splitting. Therefore, we will focus on the convective and pressure effects in order to build the numerical schemes, keeping in mind that the method can be extended to arbitrary state laws and treat cases where the RUE can be zero and the previous system degenerates toward the PGD.

3. A hybrid relaxation scheme for coupled GGD/PGD configurations

In this section, we provide the key ingredients in order to propose a global numerical strategy in 1D and 2D, able to deal with both GGD and PGD at the same time, and to handle vacuum. It is based on the concept of relaxation approximation for systems of conservation laws and the technical details of the approach are to be found in Boileau *et al.* (2010). In the following, the notations of the previous section are abandoned and replaced by the usual notations for hyperbolic systems of conservation laws.

3.1. *PGD approximated by GGD with energy relaxation and splitting*

We first propose to write the PGD par of system (2.1) under the equivalent form

$$\left\{ \begin{array}{l} \partial_t \rho + \partial_x(\rho u) = 0, \\ \partial_t(\rho u) + \partial_x(\rho u^2 + p) = 0, \end{array} \right. \tag{3.1}$$

with $p = 0$. Then, following the general idea of Coquel & Perthame (1998), we propose to approximate the solutions of this system by the ones of the energy relaxation system

$$\left\{ \begin{array}{l} \partial_t \rho + \partial_x(\rho u) = 0, \\ \partial_t(\rho u) + \partial_x(\rho u^2 + p) = 0, \\ \partial_t(\rho E) + \partial_x(\rho E u + p u) = -\lambda \rho \varepsilon, \end{array} \right. \tag{3.2}$$

where the so-called relaxation internal and total energies are related by $E = \varepsilon + 1/2\, u^2$. Importantly, the pressure p here no longer equals zero but obeys for instance a perfect gas equation of state $\rho\varepsilon = p/(\gamma - 1)$. At least formally, we observe from the last equation in (3.2) that the relaxation internal energy $\rho\varepsilon$ tends to zero as the relaxation parameter $\lambda > 0$ goes to infinity. The solutions of the relaxation system (3.2) are thus expected to provide a good approximation of the solutions of the PGD for large values of λ. Note that if we define the temperature T and the mathematical entropy S according to the second principle of thermodynamics $-T dS = d\varepsilon - p d\tau$, $\tau = 1/\rho$, where the T denotes the temperature, easy calculations lead to the expected entropy inequality $\partial_t(\rho S) + \partial_x(\rho S u) = -\lambda\rho\varepsilon \leq 0$.

The numerical procedure we are going to propose in order to approximate the solutions of the pressureless gas dynamics system (2.1) is very classical in the context of relaxation approximations. It is based on an operator splitting for (3.2) and is made of two steps that we now briefly describe.

1^{rst} step: We solve the convective part of the left hand side, which is nothing but the

GGD system, also written in its abstract form:

$$\left\{\begin{array}{l}\partial_t\rho+\partial_x(\rho u)=0,\\ \partial_t(\rho u)+\partial_x(\rho u^2+p)=0,\\ \partial_t(\rho E)+\partial_x(\rho E u+pu)=0,\end{array}\right. \quad\Longleftrightarrow\quad \partial_t\mathcal{U}+\partial_x\mathcal{F}(\mathcal{U})=0. \tag{3.3}$$

2^{nd} step: In the second step, the contribution of the stiff relaxation source term is accounted for by solving the following ODE system in the asymptotic regime $\lambda\to\infty$

$$\left\{\begin{array}{l}\partial_t\rho=0\\ \partial_t(\rho u)=0\\ \partial_t(\rho E)=-\lambda\rho\varepsilon\end{array}\right. \quad\Longleftrightarrow\quad \left\{\begin{array}{l}\partial_t\rho=0\\ \partial_t(\rho u)=0\\ \partial_t\varepsilon=-\lambda\varepsilon\end{array}\right. \tag{3.4}$$

This amounts to keep ρ and ρu unchanged and to set $\varepsilon=0$, i.e. $\rho E=\frac{1}{2}\rho u^2$ and $p=0$.

3.2. *A pressure relaxation model for GGD and analytical Riemann problem resolution*

We have seen that the only non-trivial of the previous steps is the resolution of the GGD; besides, we need a numerical scheme in order to solve system (2.2), the right hand side of which is exactly the GGD. Thus we propose a pressure relaxation system as well as the exact resolution of the corresponding Riemann problem in order to approximate the solutions of the GGD system (3.3) and properly handle zero pressure and zero density. Motivated by the seminal work of Jin & Xin (1995) and Suliciu (1998), we propose to relax the nonlinearities associated with the pressure law p only, and to retain the other ones for the sake of accuracy. With this in mind, we introduce the following non linear first order system with singular perturbation:

$$\left\{\begin{array}{l}\partial_t\rho+\partial_x(\rho u)=0,\\ \partial_t(\rho u)+\partial_x(\rho u^2+\Pi)=0,\\ \partial_t(\rho E)+\partial_x(\rho E u+\Pi u)=0,\\ \partial_t(\rho\Pi)+\partial_x(\rho\Pi u+a^2u)=\mu\rho(p-\Pi),\end{array}\right. \quad\Longleftrightarrow\quad \partial_t\mathcal{V}+\partial_x\mathcal{G}(\mathcal{V})=\mu\mathcal{R}(\mathcal{V}) \tag{3.5}$$

As μ goes to infinity, we observe at least formally that the relaxation pressure Π tends to p so that the equilibrium system (3.3) is recovered in this asymptotic regime. The additional equation associated with Π is easily seen to be equivalent to $\partial_t\Pi+u\,\partial_x\Pi+\frac{a^2}{\rho}\partial_x u=\mu(p-\Pi)$. This equation is very similar to the one associated with the exact pressure p given by $\partial_t p+u\partial_x p+\rho c^2\partial_x u=0$. The choice of the parameter $a>0$ is crucial for the stability of the relaxation procedure and is determined by the so-called sub-characteristic condition $a>\rho c$ where c denotes the sound speed. The first-order system extracted from (3.5) is hyperbolic and admits the following three eigenvalues, $\lambda_1=u-a/\rho,\quad \lambda_2=u,\quad \lambda_3=u+a/\rho$, with second-order multiplicity for λ_2. We note that λ_1 and λ_3 approximate the characteristic speeds $u-c$ and $u+c$ of (3.3). Importantly, these eigenvalues are now associated with linearly degenerate characteristic fields. This implies that the Riemann problem associated with (3.5) (with $\mu=0$) can be explicitly solved, unlike the one associated with (3.3). Riemann solutions being the key ingredient to devise Godunov-type methods, this mathematical property justifies the introduction of the relaxation model (3.5). Here again, the proposed numerical procedure to approximate the solutions of the GGD system (3.3) is based on an operator splitting for (3.5) and is made of two steps:

1^{rst} step: We solve the convective part of the relaxation model with $\mu=0$ in (3.5):

$$\partial_t\mathcal{V}+\partial_x\mathcal{G}(\mathcal{V})=0. \tag{3.6}$$

In practice, we will use in this step a Godunov method based on the exact Riemann solution of (3.6).

2^{nd} step: We then solve $\partial_t \mathcal{V} + \partial_x \mathcal{G}(\mathcal{V}) = (0, 0, 0, \mu\rho(p - \Pi))$ in the asymptotic regime $\lambda \to \infty$. The conservative variables ρ, ρu and ρE are thus constant, while Π is set to be equal to p in this step.

For the sake of completeness, we now give the Riemann solution associated with (3.6). We propose to take a nonconstant in the Riemann solution and we choose to solve

$$\partial_t a + u\,\partial_x a = 0. \tag{3.7}$$

Recalling $\tau = 1/\rho$, the diagonal form of (3.6)-(3.7) is given by

$$\left\{\begin{array}{l} \partial_t(\Pi + au) + (u + a\tau)\partial_x(\Pi + au) = 0, \\ \partial_t(\Pi - au) + (u - a\tau)\partial_x(\Pi - au) = 0, \\ \partial_t(\Pi + a^2\tau) + u\partial_x(\Pi + a^2\tau) = 0, \\ \partial_t(\varepsilon - \frac{\Pi^2}{2a^2}) + u\partial_x(\varepsilon - \frac{\Pi^2}{2a^2}) = 0, \\ \partial_t a + u\partial_x a = 0. \end{array}\right.$$

In other words, the quantities $(\Pi \pm au)$, respectively $(\Pi + a^2\tau)$, $(\varepsilon - \frac{\Pi^2}{2a^2})$ and a, are (strong) Riemann invariants for the eigenvalues $u \pm a\tau$, resp. u. Let be given $\mathcal{V}_L = (\mathcal{U}_L, (\rho\Pi)_L)$ and $\mathcal{V}_R = (\mathcal{U}_R, (\rho\Pi)_R)$ two constant states and let a_L and a_R be two values for a. The self-similar Riemann solution $(x, t) \mapsto \mathcal{V}(x/t; \mathcal{V}_L, \mathcal{V}_R; a_L, a_R)$ associated with (3.6) and initial data $\mathcal{V}(x, t = 0) = \left\{\begin{array}{ll} \mathcal{V}_L & \text{if} \quad x < 0, \\ \mathcal{V}_R & \text{if} \quad x > 0, \end{array}\right.$ is made of four constant states $\mathcal{V}_L$, $\mathcal{V}_L^*$, $\mathcal{V}_R^*$ and $\mathcal{V}_R$, separated by three contact discontinuities associated with $\lambda_k = \lambda_k(\mathcal{V})$, $k = 1, 2, 3$ and propagating with speeds denoted by $\lambda(\mathcal{V}_L, \mathcal{V}_L^*)$, $\lambda(\mathcal{V}_L^*, \mathcal{V}_R^*)$ and $\lambda(\mathcal{V}_R^*, \mathcal{V}_R)$. The intermediate states $\mathcal{V}_L^*$, $\mathcal{V}_R^*$, as well as the speeds of propagation, are determined using for all $k = 1, 2, 3$ the continuity of the (strong) Riemann invariants for λ_k across the contact discontinuity associated with λ_l, $l \neq k$. We get after easy calculations $\lambda(\mathcal{V}_L, \mathcal{V}_L^*) = \lambda_1(\mathcal{V}_L) = u_L - a_L\tau_L$, $\lambda(\mathcal{V}_L^*, \mathcal{V}_R^*) = u^*$, $\lambda(\mathcal{V}_R^*, \mathcal{V}_R) = \lambda_3(\mathcal{V}_R) = u_R + a_R\tau_R$ and

$$u_L^* = u_R^* = u^* = \frac{a_L u_L + a_R u_R + \Pi_L - \Pi_R}{a_L + a_R}, \Pi_L^* = \Pi_R^* = \frac{a_R\Pi_L + a_L\Pi_R - a_L a_R(u_R - u_L)}{a_L + a_R},$$

$$\frac{1}{\rho_L^*} = \frac{1}{\rho_L} + \frac{a_R(u_R - u_L) + \Pi_L - \Pi_R}{a_L(a_L + a_R)}, \quad \frac{1}{\rho_R^*} = \frac{1}{\rho_R} + \frac{a_L(u_R - u_L) + \Pi_R - \Pi_L}{a_R(a_L + a_R)},$$

$$\varepsilon_L^* = \varepsilon_L - \frac{\Pi_L^2}{2a_L^2} + \frac{\Pi^{*2}}{2a_L^2}, \quad \varepsilon_R^* = \varepsilon_R - \frac{\Pi_R^2}{2a_R^2} + \frac{\Pi^{*2}}{2a_R^2}.$$

At this stage, the initial states $\mathcal{V}_L$ and $\mathcal{V}_R$ and more precisely the free parameters a_L and a_R are implicitly assumed to be such that the waves in the Riemann solutions are ordered as they should, namely

$$\lambda_1(\mathcal{V}_L) = u_L - \frac{a_L}{\rho_L} < u^\star < \lambda_3(\mathcal{V}_R) = u_R + \frac{a_R}{\rho_R}. \tag{3.8}$$

Following Bouchut (2004), we define $a_L = a_L(\mathcal{V}_L)$ and $a_R = a_R(\mathcal{V}_R)$ as follows:

$$\text{if} \quad p_R \geq p_L \left\{\begin{array}{l} a_L/\rho_L = \max(c_L, c_{min}) + \alpha\left(\frac{(p_R - p_L)}{\rho_R c_R} + u_L - u_R\right)_+ \\ a_R/\rho_R = \max(c_R, c_{min}) + \alpha\left(\frac{p_L - p_R}{a_L} + u_L - u_R\right)_+, \end{array}\right.$$

$$\text{if} \quad p_R \le p_L \begin{cases} a_L/\rho_L = \max(c_L, c_{min}) + \alpha \left(\frac{p_R - p_L}{a_R} + u_L - u_R \right)_+ \\ a_R/\rho_R = \max(c_R, c_{min}) + \alpha \left(\frac{p_L - p_R}{\rho_L c_L} + u_L - u_R \right)_+ \end{cases}$$

with $\alpha = (\gamma+1)/2$, $c_{min} > 0$, where $p_{L,R} = p_{L,R}(\mathcal{U}_{L,R})$, $c_{L,R} = c_{L,R}(\mathcal{U}_{L,R})$ are the values of the pressures and sound speeds evaluated on $\mathcal{U}_L$ and $\mathcal{U}_R$ and where $(\ )_+$ denotes the positive part of a quantity. This choice has several advantages. First, it is shown to fullfil (3.8) and to give the positivy of the intermediate densities ρ_L^* and ρ_R^*. Then, it complies with the sub-characteristic condition $a > \rho c$. At last, it guarantees the nonlinear stability of the underlying relaxation scheme that will be described in the next paragraph, and the possibility of handling vacuum in the sense that the speeds of propagation $\lambda_1(\mathcal{V}_L)$ and $\lambda_3(\mathcal{V}_R)$ remain finite. In particular, discrete entropy inequalities as well as maximum principles can be proved. These results are pretty technical to establish and are not presented in this paper. We refer the reader to Bouchut (2004) for the details. In the case of PGD, these formulas are to be considered with $p_L = p_R = 0$ and $c_L = c_R = 0$. We then observe that the threshold c_{min} allows to guarantee (3.8) when $u_L \le u_R$ and then to avoid the resonance phenomenon. We thus are able to provide an analytical solution of the Riemann problem in the whole range of density and pressures without having problems with singular limits.

3.3. *A generic finite volume relaxation scheme for gas dynamics and PGD separately*

In this paragraph, based on the previous results, we present a finite volume relaxation scheme for approximating the solutions of the GGD or PGD equations (3.3) and (3.2) separately but exactly along the same lines and using the same formalism. This will allow an easy coupling in the case of mixed computations involving both GGD and PGD at the same time in the next paragraph. Just note that in the pressureless case, E must be understood as a function of the unknowns ρ and ρu, namely $E = (\rho u)^2/2\rho$, but not as an unknown with evolution given by the passive transport equation $\partial_t(\rho E) + \partial_x(\rho E u) = 0$. Initial condition is denoted $\mathcal{U}(x,0) = \mathcal{U}_0(x)$, with $E_0(x) = (\rho u)_0^2(x)/2\rho_0(x)$ in the case of PGD.

Let Δx and Δt be two constant steps for space and time discretizations. Let $(x_j)_{j\in\mathbb{Z}}$ be a sequence of equidistributed points in $\mathbb{R}$: $x_{j+1} - x_j = \Delta x$. For all $j \in \mathbb{Z}$ and all $n \in \mathbb{N}$, we define $x_{j+1/2} = x_j + \Delta x/2$, $t^n = n\Delta t$, and consider the following discretization of the computational domain $\mathbb{R}_x \times \mathbb{R}_t^+ = \bigcup_{j\in\mathbb{Z}} \bigcup_{n\ge 0} C_j^n$, with $C_j^n = [x_{j-1/2}, x_{j+1/2}[\times[t^n, t^{n+1}[$. On the one hand and as usual in the context of finite volume methods, the approximate solution $\mathcal{U}_{\Delta t,\Delta x}(x,t)$ of (3.2) with initial data $\mathcal{U}_0$ is sought as a piecewise constant function on each slab C_j^n: $\mathcal{U}_{\Delta t,\Delta x}(x,t) = \mathcal{U}_j^n$ for $(x,t) \in C_j^n$. At time $t = 0$, we set $\mathcal{U}_j^0 = \frac{1}{\Delta x}\int_{x_{j-1/2}}^{x_{j+1/2}} \mathcal{U}_0(x)dx$, $j \in \mathbb{Z}$. On the other hand, we define from $\mathcal{U}_{\Delta t,\Delta x}$ the piecewise constant approximate solution $\mathcal{V}_{\Delta t,\Delta x}(x,t) = \mathcal{V}_j^n = \left(\mathcal{U}_j^n, (\rho\Pi)_j^n\right)$ for $(x,t) \in C_j^n$. This solution is set to be at *equilibrium*, that is $(\rho\Pi)_j^n = p(\mathcal{U}_j^n)$, for the GGD and $(\rho\Pi)_j^n = 0$, for the PGD. Let us assume that the solution $\mathcal{U}_{\Delta t,\Delta x}(x,t^n)$ at time t^n is known. In order to advance it to the next time level t^{n+1}, we now describe the two steps of the method in details.

1^{rst} step: evolution in time $(t^n \to t^{n+1-})$

In this step, we solve (3.6) with $\mathcal{V}_{\Delta t,\Delta x}(x,t^n)$ as initial data and for times $t \in [0, \Delta t]$. Under the CFL condition $\Delta t/\Delta x \max_{\mathcal{V}}(|\lambda_i(\mathcal{V})|, i = 1,2,3) < \frac{1}{2}$ where the maximum is taken over all the $\mathcal{V}$ under consideration, the solution is obtained by solving a sequence of non interacting Riemann problems set at each cell interface $x_{j+1/2}$. It is explicitly known

by the previous paragraph and we have

$$\mathcal{V}(x,t) = \mathcal{V}(\tfrac{x-x_{j+1/2}}{t}; \mathcal{V}_j^n, \mathcal{V}_{j+1}^n; a_L(\mathcal{V}_j^n), a_R(\mathcal{V}_{j+1}^n)), \quad (x,t) \in [x_j, x_{j+1}]\times]0,\Delta t], j \in \mathbb{Z}.$$

Using the Godunov method, the update formula can be easily given under the conservation form $\mathcal{V}_j^{n+1-} = \mathcal{V}_j^n - \Delta t/\Delta x(g(\mathcal{V}_j^n, \mathcal{V}_{j+1}^n) - g(\mathcal{V}_{j-1}^n, \mathcal{V}_j^n))$, $j \in \mathbb{Z}$, $n \geq 0$, where the numerical flux function, which is explicitly known, writes for all $j \in \mathbb{Z}$

$$g(\mathcal{V}_j^n, \mathcal{V}_{j+1}^n) = \mathcal{G}\Big(\mathcal{V}\big(0; \mathcal{V}_j^n, \mathcal{V}_{j+1}^n; a_L(\mathcal{V}_j^n), a_R(\mathcal{V}_{j+1}^n)\big)\Big). \tag{3.9}$$

2^{nd} step: relaxation $(t^{n+1-} \to t^{n+1})$
We now project the solution $\mathcal{V}_{\Delta t,\Delta x}(x, t^{n+1-})$ obtained at the end of the previous step on the equilibrium manifold $\mu = +\infty$: $\quad \mathcal{V}_j^{n+1} = \big(\mathcal{U}_j^{n+1}, (\rho\Pi)_j^{n+1}\big) \quad$ for all $\quad j \in \mathbb{Z}$

$$\text{with} \quad \begin{cases} \mathcal{U}_j^{n+1} = \mathcal{U}_j^{n+1-} \quad \text{and} \quad (\rho\Pi)_j^{n+1} = p(\mathcal{U}_j^{n+1}) \quad \text{for the GGD} \\ \mathcal{U}_j^{n+1} = \big(\rho, \rho u, (\rho u)^2/2\rho\big)_j^{n+1-} \text{ and} \quad (\rho\Pi)_j^{n+1} = 0 \quad \text{for the PGD} \end{cases}$$

In agreement with the description of these two steps, the approximate solution $\mathcal{U}_{\Delta t,\Delta x}$ is then updated according to the following consistent finite volume method:

$$\rho_j^{n+1} = \rho_j^n - \frac{\Delta t}{\Delta x}\Delta f^{\rho}(\mathcal{U}_{j-1}^n, \mathcal{U}_j^n, \mathcal{U}_{j+1}^n), \quad (\rho u)_j^{n+1} = (\rho u)_j^n - \frac{\Delta t}{\Delta x}\Delta f^{\rho u}(\mathcal{U}_{j-1}^n, \mathcal{U}_j^n, \mathcal{U}_{j+1}^n), \tag{3.10}$$

$$\text{together with } (\rho E)_j^{n+1} = (\rho E)_j^n - \frac{\Delta t}{\Delta x}\Delta f^{\rho E}(\mathcal{U}_{j-1}^n, \mathcal{U}_j^n, \mathcal{U}_{j+1}^n) \text{ for the GGD} \tag{3.11}$$

$$(\rho E)_j^{n+1} = \left(\frac{(\rho u)^2}{2\rho}\right)_j^{n+1} \quad \text{for the PGD.} \tag{3.12}$$

Here of course, $(f^{\rho}, f^{\rho u}, f^{\rho E})(\mathcal{U}_j^n, \mathcal{U}_{j+1}^n)$ denote the first three components of $g(\mathcal{V}_j^n, \mathcal{V}_{j+1}^n)$ and $\Delta f^{\alpha}(\mathcal{U}_{j-1}^n, \mathcal{U}_j^n, \mathcal{U}_{j+1}^n) = f^{\alpha}(\mathcal{U}_j^n, \mathcal{U}_{j+1}^n) - f^{\alpha}(\mathcal{U}_{j-1}^n, \mathcal{U}_j^n)$ for $\alpha = \rho, \rho u, \rho E$.

3.4. *Coupling the GGD and PGD by the use of an internal energy threshold*

In order to perform computations involving both GGD and PGD at the same time, we have to couple the relaxation schemes developed for both systems. The main difference then clearly lies in the treatment of the energy equation. For the sake of clarity, we begin by introducing a color function Y such that $Y = 1$ for GGD and $Y = 0$ for PGD. From a numerical point of view, a given cell $\mathcal{C}_j^n$ is said to be *pressureless*, or equivalently such that $Y_j^n = 0$, if the internal energy $\varepsilon_j^n = (\rho E - \frac{(\rho u)^2}{2\rho})_j^n$ is less than a given threshold ε_{min} and *with pressure*, that is $Y_j^n = 1$, otherwise. Introducing the threshold ε_{min} is a convenient way to switch from one algorithm to the other. In agreement with the threshold c_{min} already introduced for the sound speed in the definition of a_L and a_R, we set $\varepsilon_{min} = \frac{c_{min}^2}{\gamma(\gamma-1)}$. We thus distinguish between zones with PGD where the internal energy is exactly zero and zones where the energy level is above the defined small threshold, a property which is preserved by the pure convective part of the evolution. Let us consider a given cell $\mathcal{C}_j^n$. Two different situations must be distinguished, depending in particular on whether $Y_{j-1}^n = Y_j^n = Y_{j+1}^n$ or not. *The case* $Y_{j-1}^n = Y_j^n = Y_{j+1}^n$. In this case, we simply use (3.10) and (3.12) without any modification. *The case* $Y_{j-1}^n \neq Y_j^n$ *and/or* $Y_{j+1}^n \neq Y_j^n$. In this case, we consider that the cell $\mathcal{C}_j^n$ should be considered *with pressure* in the update formula. Thus we propose to use Eq. (3.10-3.12) where for

$k = j-1, j, j+1$, we replace the $\mathcal{U}^n$ by $\overline{\mathcal{U}}^n$ and ρE_k^n by $\overline{\rho E}_k^n$, with :

$$\begin{cases} \overline{\mathcal{U}}_k^n = (\rho, \rho u, \overline{\rho E})_k^n, \quad \overline{\rho E}_k^n = \rho_k^n \varepsilon_{min} + \left((\rho u)^2/(2\rho)\right)_k^n & \text{if} \quad \varepsilon_k^n < \varepsilon_{min} \\ \overline{\mathcal{U}}_k^n = \mathcal{U}_k^n \quad \text{otherwise.} \end{cases}$$

The interface between PGD and GGD is automaticaly treated by means of a threshold. The GGD zone can propagate and, with $\varepsilon_t = 0$ as energy source, eventually vanish.

3.5. *Extension to 2D configurations and to second-order accuracy*

The $2D$ computations on cartesian meshes presented in the next section are performed using a very classical dimensional splitting method. Recall that if we denote (u, v) the two components of the velocity field, v being associated with the additional space dimension, the governing equation for v in the quasi-$1D$ system reads

$$\partial_t(\rho v) + \partial_x(\rho v u) = 0. \tag{3.13}$$

This equation means that v is simply passively transported with the flow. From a numerical point of view, a natural discretisation of (3.13) is given by :

$$\begin{aligned} (\rho v)_j^{n+1} &= (\rho v)_j^n - \frac{\Delta t}{\Delta x} \Delta f^{\rho v}(\mathcal{U}_{j-1}^n, \mathcal{U}_j^n, \mathcal{U}_{j+1}^n), \\ \Delta f^{\rho v}(\mathcal{U}_{j-1}^n, \mathcal{U}_j^n, \mathcal{U}_{j+1}^n) &= f^{\rho v}(\mathcal{U}_j^n, \mathcal{U}_{j+1}^n) - f^{\rho v}(\mathcal{U}_{j-1}^n, \mathcal{U}_j^n), \\ f^{\rho v}(\mathcal{U}_j^n, \mathcal{U}_{j+1}^n) &= \begin{cases} f^{\rho}(\mathcal{U}_j^n, \mathcal{U}_{j+1}^n)\ v_j^n & \text{if} \quad f^{\rho}(\mathcal{U}_j^n, \mathcal{U}_{j+1}^n) \geq 0, \\ f^{\rho}(\mathcal{U}_j^n, \mathcal{U}_{j+1}^n)\ v_{j+1}^n & \text{if} \quad f^{\rho}(\mathcal{U}_j^n, \mathcal{U}_{j+1}^n) \leq 0. \end{cases} \end{aligned}$$

This formula has been first introduced in Larrouturou (1991) and complies with the exact resolution of the Riemann problem for the quasi-$1D$ relaxation model. The calculations are left to the reader. The space second-order extension we use in the numerical experiments is based on a classical MUSCL reconstruction technique on the primitive variables ρ, u and ε, using a minmod slope limiter and a second order Runge-Kutta method.

4. Results and discussion

In order to evaluate the hybrid PGD/GGD relaxation method, the Sod shock tube test is performed with the initial conditions $\left(v^0 = 0, \rho^0 = 1, p^0 = 1.1 \,|\, x \leq 0.5\right)$ and $\left(v^0 = 0, \rho^0 = 0.125, p^0 = 0 \,|\, x > 0.5\right)$. At the initial time, $x > 0.5$ is a zero pressure field computed with the PGD algorithm while $x \leq 0.5$ is computed with the GGD algorithm. In this test case as in all other coupled method calculations, $c_{min} = 10^{-5}$ and $\varepsilon_{min} = 10^{-10}$. Figures 1 shows the density and pressure profiles at time $t = 0.1644$ for the first and second order relaxation schemes. Due to the poor discretization of the surface discontinuity and the shock, the density solution is smeared by the numerical diffusion. The second order scheme presents a significantly better accuracy than the first order one. While the shock propagates toward the pressureless region, the interface between pressure and pressureless regions does not present any numerical artefact. However, numerical diffusion causes some pressureless cells to become with pressure in the upstream region of the shock, this effect being stronger with the first order scheme. For brevity, other 1D tests that proves the high robustness of the method, in particular in a shock/δ-shock interaction, are not shown here (see Boileau *et al.* (2010)).

Figure 2.a shows the velocity field of the carrier phase corresponding to the four contra-rotating Taylor-Green vortices used in the following numerical tests. The spray dynamics is coupled to the gaseous flow field through a Stokes drag source term in the momentum

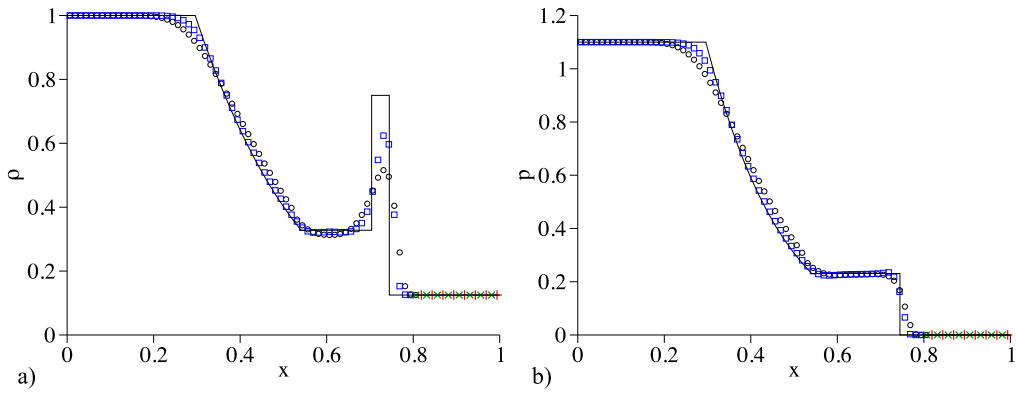

FIGURE 1. Profiles of density (a) and pressure (b) for the hybrid relaxation scheme in Sod numerical test at time $t = 0.1644$: analytical solution (—), 1^{rst} order relaxation scheme (pressure region: ∘, pressureless region: +), 2^{nd} order relaxation scheme (pressure region: □, pressureless region: ×) (80 nodes, CFL = 0.5).

equation, which amounts to relaxing the spray velocity field toward the gaseous one at a rate set by the Stokes number St, i.e. the non dimensional relaxation time. From de Chaisemartin (2009) we know that there exists a critical value $\mathrm{St}_c = 1/8\pi$ which separates two regimes. For $\mathrm{St} < \mathrm{St}_c$, the particles cannot escape from the Taylor-Green vortices while, for $\mathrm{St} \geq \mathrm{St}_c$, they are ejected out of their original vortices. Therefore, we have conducted various tests with two values of St in order to cover these two regimes: $\mathrm{St} = 0.9\mathrm{St}_c$ and $\mathrm{St} = 13\mathrm{St}_c$ (Boileau *et al.* (2010)). In the following we only present the latter case. From a numerical point of view, the drag source term $\overline{\mathbf{F}}$ is applied via operator splitting through an analytical expression of the exponential relaxation (Eq. 2.2). The initial spray velocity is uniformly zero for all test-cases.

In order to test the capability of the method to treat multidimensional transport of inertial particles, the Stokes number is fixed at a supercritical value $\mathrm{St} = 13\mathrm{St}_c$. Figure 2.a shows the initial density distribution provided by a cardinal sinus function. To allow comparison with Bouchut's scheme, the pressureless relaxation scheme is used. Figure 2.b and 2.c show the results at time $t = 0.8$ for the second order Bouchut scheme and the second order relaxation scheme. Both schemes predict very similar density fields featuring a δ-shock, as expected (see de Chaisemartin (2009)).

The hybrid scheme is evaluated in a configuration where two parcels of high-inertia particles are ejected from their initial vortices and collide. The density distribution is given by a cardinal sinus function whose center is $(0.125, \pm 0.375)$ and radius 0.125 (see Fig. 3). A PGD calculation and a GGD calculation are performed. For the GGD case, a relaxation term of internal energy is imposed using a cardinal sine function centered on $y = 0$ with a radius of 0.125 and a maximum value of $\varepsilon_t = 0.5$ (see Fig. 3.c). This energy source term simulates the effect of a local turbulence region of the carrier flow on the particles transport. As expected, Fig. 3 shows that, for both PGD and hybrid schemes, each particle parcel is ejected from its vortex and start to interact with its mirror image at $t = 0.75$. In the PGD case (Fig. 3.a), this interaction forms a δ-shock at the meeting line $y = 0$. On the other hand, the hybrid case (Fig. 3.c) features only a small increase in density at $y = 0$ because pressure effects limit the concentration of particles. Later, the behavior of both schemes are even more different (see Fig. 3.b and d). Most of the density is concentrated close to $y = 0$ in the PGD case, while a smoother density distribution is

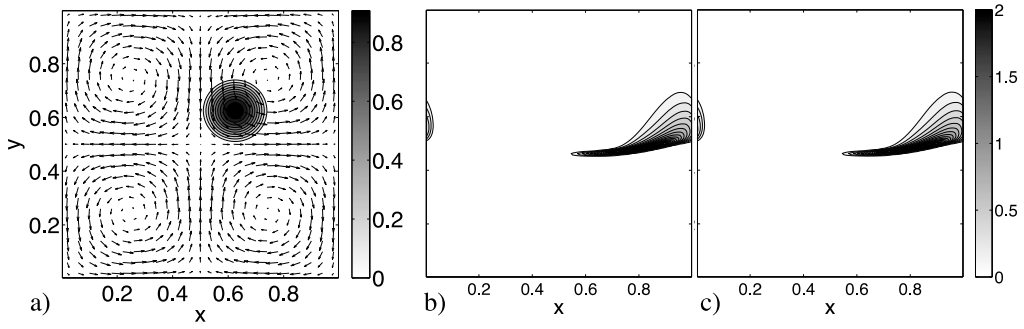

FIGURE 2. Carrier phase velocity field (Taylor-Green periodic vortices) and initial density contours (a). Snapshots of the density distribution at time $t = 0.8$ for Stokes number $\mathrm{St} = 13\mathrm{St}_c$ (200 nodes, CFL = 1): 2^{nd} order Bouchut scheme (b) and 2^{nd} order pressureless relaxation scheme (c).

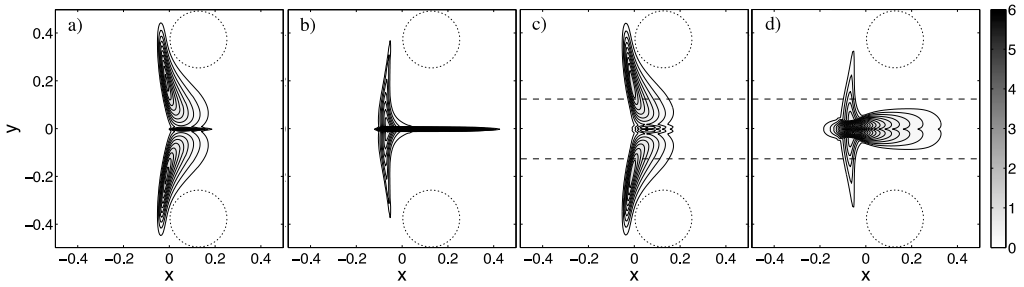

FIGURE 3. Snapshots of the density for Stokes number $\mathrm{St} = 13\mathrm{St}_c$ (1^{rst} order relaxation scheme, 200 nodes, CFL = 1): pressureless scheme (a, b) and hybrid scheme (c, d). Time $t = 0.75$ (a, c) and $t = 1.1$ (b, d). Dotted circles and dashed lines are the limits of the cardinal sinus function of the initial density distribution and the energy source term (b, d) respectively.

observed in the hybrid case. Note that with the hybrid scheme, the maximum of density is not located on the $y = 0$ line because the pressure gradient resulting from the energy source term prevents particles from accumulating.

A novel hybrid numerical method for solving Eulerian models for spray dynamics has been proposed. Based on the relaxation method, it can deal with both PGD and GGD system of equations in various zones of the same configuration. Therefore, it has the ability, on the one hand, to compute the low-inertia particles dynamics – described by PGD – and, on the other hand, to account for the effects of high-inertia particles in the turbulent regions of the flow — falling under the general GGD framework. The zero-density is also explicitely handled, which is a key feature for simulating spray injection. In terms of accuracy, two-dimensional tests in PGD configurations show that the scheme matches the kinetic scheme of Bouchut previously used and thus validate the approach. Beside, the hybrid PGD/GGD approach predicts accurate results in the 1D shock tube test-case. Two-dimensional simulations in the framework of Taylor-Green vortices with eventually localized turbulent subgrid energy source allow to exhibit the potential of the method. Besides, the relaxation framework makes it possible to handle arbitrary pressure law such as the real gas-type behaviour of turbulent sprays. Therefore the present investigation shows that this method provides the ingredients needed to simulate turbulent sprays in a DNS/LES framework.

Acknowledgements

Quang Huy Tran from IFP is gratefully acknowledged for his precious help. The authors wish to thank also the Center for Turbulence Research at Stanford University for hospitality, financial and technical support.

REFERENCES

Berthon, C., Breuss, M. & Titeux, M.O. 2006 A relaxation scheme for the approximation of the pressureless Euler equations. *Numer. Methods for Partial Differential Equations* **22** (2), 484–505.

Boileau, M., Chalons, C., Laurent, F., De Chaisemartin, S. & Massot, M. 2010 Robust numerical schemes for Eulerian spray DNS and LES in two-phase turbulent flows. In preparation for *SIAM J. Sci. Comput.*, preliminary version available in *Proc. 7th Int. Conf. Multiphase Flow, Tampa, FL, USA - 2010*.

Boileau, M., Staffelbach, G., Cuenot, B., Poinsot, T. & Bérat, C. 2008 LES of an ignition sequence in a gas turbine engine. *Combust. Flame* **154** (1–2), 2–22.

Bouchut, F. 2004 *Nonlinear stability of finite volume methods for hyperbolic conservation laws, and well-balanced schemes for sources*. Frontiers in Mathematics series.

de Chaisemartin, S. 2009 Modèles eulériens et simulation numérique de la dispersion turbulente de brouillards qui s'évaporent. PhD thesis, Ecole Centrale Paris, France.

Coquel, F. & Perthame, B. 1998 Relaxation of energy and approximate riemann solvers for general pressure laws in fluid dynamics. *SIAM J. Numer. Anal.* **35** (6), 2223–2249.

Fevrier, P., Simonin, O. & Squires, K. 2005 Partitioning of particle velocities in gas-solid turbulent flows into a continuous field and a spatially uncorrelated random distribution theoretical formalism and numerical study. *J.Fluid Mech* **533**, 1–46.

Freret, L., Thomine, O., Reveillon, J., de Chaisemartin, S., Laurent, F. & Massot, M. 2011 On the role of preferential segregation in flame dynamics in polydisperse evaporating sprays. In *Proceedings of the Summer Program 2010, Center for Turbulence Research, Stanford University*, pp. 1–10.

Jin, S. & Xin, Z. 1995 The relaxation schemes for systems of conservation laws in arbitrary space dimensions. *Comm. Pure Appl. Math.* **48** (3).

Kaufmann, A., Moreau, M., Simonin, O. & Helie, J. 2008 Comparison between Lagrangian and mesoscopic Eulerian modelling approaches for inertial particles suspended in decaying isotropic turbulence. *J. Comput. Phys.* **227** (13), 6448 – 6472.

Larrouturou, B. 1991 How to preserve the mass fractions positivity when computing compressible multi-component flows. *J. Comput. Phys.* **95**, 59–84.

Riber, E., Moreau, M., Simonin, O. & Cuenot, B. 2005 Towards large eddy simulation of non-homogeneous particle laden turbulent gas flows using euler-euler approach. In *11th Workshop on Two-Phase Flow Predictions, Merseburg, Germany*.

Suliciu, I. 1998 Energy estimates in rate-type thermo-viscoplasticity. *Int. J. Plast.* **14**, 227–244.

Vié, A., Sanjosé, M., Jay, S., Angelberger, C., Cuenot, B. & Massot, M. 2010 Evaluation of a multifluid mesoscopic eulerian formalism on the Large Eddy Simulation of an aeronautical-type configuration. In *Proc. 7th Int. Conf. Multiphase Flow, Tampa, FL, USA*.